Jurnal Teknologi

Full Paper

MACHINABILITY AND PHASE TRANSFORMATION TEMPERATURES OF MARTENSITIC AND AUSTENITIC NITI SHAPE MEMORY ALLOYS IN DRY AND CHILLED AIR MACHINING

Muhammad Hisyamuddin Rosli[a]*, Zainal Abidin Zailani[a,b], Norshah Afizi Shuaib[a,c]

[a]Faculty of Mechanical Engineering and Technology, Universiti Malaysia Perlis, 02600 Arau, Perlis, Malaysia
[b]Sustainable Manufacturing Technology Research Group, Faculty of Mechanical Engineering and Technology, Universiti Malaysia Perlis, 02600 Arau, Perlis, Malaysia
[c]Green Design and Manufacture Research Group, Center of Excellence Geopolymer & Green Technology (CEGeoGTech), Universiti Malaysia Perlis, 01000 Kangar, Perlis, Malaysia

Article history
Received
3 March 2025
Received in revised form
31 May 2025
Accepted
3 June 2025
Published Online
27 February 2026

*Corresponding author
muhammadhisyamuddinbin-rosli@studentmail.unimap.edu.my

Graphical abstract

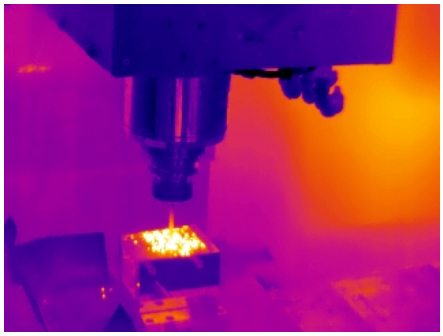

Abstract

This study investigates the effects of dry and chilled air milling on the machinability and phase transformation behaviour of martensitic and austenitic nickel-titanium (NiTi) alloys. NiTi alloys are widely used in biomedical and automotive industries for their shape memory effect and super-elasticity; however, their high ductility and temperature sensitivity pose machining challenges, leading to severe tool wear and poor surface quality. Key machinability aspects including cutting force, tool wear, burr formation, and surface roughness, were analysed alongside phase transformation characteristics using Differential Scanning Calorimetry (DSC). Results show that chilled air cutting significantly reduces cutting force for austenitic NiTi but has a limited effect on martensitic NiTi. It also lowers cutting temperatures to 40°C, enhances tool wear resistance, and minimises burr formation. Chilled air cutting also improved surface roughness by 50% and 20% for martensitic and austenitic NiTi, respectively. While neither cutting condition fully preserved NiTi transformation curves, chilled air cutting promoted the inhibition of multi-peak appearances in martensitic NiTi, potentially improving phase stability.

Keywords: Milling, chilled air, nickel titanium, tool wear, phase transformation

Abstrak

Kajian ini menyiasat kesan pemesinan secara kering dan secara berudara sejuk ke atas kebolehmesinan dan kelakuan transformasi fasa aloi nikel-titanium (NiTi) martensit dan austenit. Aloi NiTi digunakan secara meluas dalam industri bioperubatan dan automotif kerana kesan ingatan bentuk dan keanjalan supernya. Walau bagaimanapun, kemuluran dan kepekaan suhu yang tinggi menimbulkan cabaran pemesinan, yang membawa kepada haus alat yang teruk dan kualiti permukaan yang rendah. Aspek kebolehmesinan utama termasuk daya pemesinan, haus alatan, pembentukan gerigis, dan kekasaran permukaan, telah dianalisis bersama ciri-ciri transformasi fasa menggunakan Kalorimetri Pengimbasan Kebezaan (DSC). Keputusan menunjukkan bahawa pemesinan berudara sejuk mengurangkan daya pemotongan dengan ketara untuk NiTi austenit tetapi mempunyai kesan terhad pada NiTi martensit. Ia juga merendahkan suhu pemotongan kepada 40°C, meningkatkan rintangan haus alat, dan meminimumkan pembentukan gerigis. Pemesinan berudara sejuk juga menghasilkan penambahbaikan terhadap kekasaran permukaan sebanyak 50% dan 20% masing-masing untuk NiTi martensit dan austenit. Walaupun kedua-dua keadaan pemesinan tidak mengekalkan lengkung transformasi NiTi sepenuhnya, pemesinan berudara sejuk menyumbang pada perencatan penampilan puncak berbilang dalam NiTi martensit, yang berpotensi meningkatkan kestabilan fasa.

Kata kunci: Pemesinan, udara sejuk, nikel titanium, haus alat, transformasi fasa

1.0 INTRODUCTION

Nickel-titanium (NiTi) alloys are widely recognised for their unique properties, particularly the shape memory effect (SME) and super-elasticity (SE) [1]. SME is characterised by NiTi alloys' ability to return to their original shape after deformation, while SE refers to their ability to withstand significant mechanical stress without permanent deformation. NiTi alloys exist in two distinct phases: martensitic and austenitic. The martensitic phase, occurring at low temperatures, is characterised by its soft and ductile nature, which allows it to undergo large strains under stress. This phase is advantageous for biomedical applications, requiring high flexibility and mechanical adaptability [2]. Conversely, the austenitic phase, which forms at higher temperatures, exhibits increased strength and rigidity, essential for applications requiring high mechanical performance [3], [4]. This transition between martensitic and austenitic phases of NiTi's crystal structure is fundamental to the alloy's unique properties of SME and SE.

The milling process of NiTi is important in manufacturing precision components for high-performance applications, particularly in the biomedical, aerospace, and automotive industries. The unique properties of NiTi alloys of SME and SE make them useful in applications like medical devices (e.g., stents, orthodontic wires), actuators, and safety systems in automotive engineering [5], [6], [7]. However, these properties pose significant challenges during machining, as NiTi alloys exhibit high ductility and low thermal conductivity and are highly sensitive to temperature fluctuations [8]. These machining challenges often result in complications such as excessive tool wear, poor surface finish and burr formation, and dimensional inaccuracies [9], [10]. As such, gaining understanding of the milling process of NiTi is essential for mitigating those complications. With mitigated outcomes, such as improved surface finish and dimensional accuracy, functional reliability of machined NiTi components could be achieved.

Machining of alloys typically involves flood lubrication, where cutting oils are applied to reduce friction, dissipate heat, and prolong tool life [11]. Flood lubrication has long been considered an effective method for controlling cutting temperatures and improving tool performance. However, the widespread use of cutting fluids has raised environmental, economic, and health concerns [12]. From an ecological perspective, the disposal of used cutting oils presents significant challenges due to their hazardous nature, contributing to industrial waste and pollution [13]. The economic burden of purchasing and maintaining these fluids and associated disposal costs can be substantial. Furthermore, long-term exposure to cutting fluids can result in health issues such as respiratory and skin problems, which pose a significant risk to machinists [14]. As such, while flood lubrication continues to be a common practice in machining, the associated drawbacks have spurred interest in exploring alternative methods.

In contrast, dry cutting, which involves machining without cutting fluids, has emerged as a more environmentally friendly and cost-effective alternative [15]. Dry cutting eliminates the environmental impact of cutting fluid disposal, offering a more sustainable approach to machining. However, dry cutting presents challenges, particularly in machining difficult-to-cut materials like NiTi alloys.

The absence of cutting fluids leads to higher cutting temperatures, increased tool wear, and more severe surface degradation, including the formation of burrs and poor surface finishes [10]. The lack of adequate cooling in dry-cutting processes causes extreme levels of heat generation, further exacerbating these issues [16].

In recent years, chilled air cooling has emerged as a promising alternative capable of mitigating extreme levels of heat generation during machining, offering better cooling options than dry cutting. Chilled air cooling uses a vortex tube that produces low-temperature air to cool the cutting zone, thereby reducing the heat generated during machining [17]. This technique offers several advantages over traditional cutting oils. Environmentally, chilled air cooling eliminates the need for harmful cutting fluids, reducing waste and pollution [18]. Chilled air cooling eliminates the health risks of cutting fluids, making it a safer option for machinists. Moreover, it has effectively reduced cutting temperatures, improved tool life, reduced tool wear, and enhanced surface finish quality [19] [20].

Despite extensive studies on the machining of NiTi, there is limited research focusing specifically on understanding the effects of chilled air-cooling on NiTi, especially in terms of its machinability and phase transformation behaviour for both martensitic and austenitic NiTi side by side, which remains narrowly discussed and compared. To fill this gap, the present study aims to gain deeper insights into the milling effects towards machinability and NiTi transformation behaviour for both types of NiTi, namely martensitic and austenitic NiTi. The research focuses on evaluating the machining impacts on the cutting force, tool wear, surface roughness, and burr formation, as well as understanding the phase transformation behaviour through differential scanning calorimetry investigation.

2.0 METHODOLOGY

2.1 Experimental Setup and Machining Conditions

The workpieces for the experiments comprised of two varieties of NiTi bar: martensitic NiTi and austenitic NiTi, which exhibit as martensitic and austenitic phases at room temperature, respectively. Both types of workpieces have the same dimensions, measuring 80 mm × 20 mm × 3 mm (length × width × height). The as-received NiTi workpiece's chemical composition was confirmed through micro-X-ray fluorescence (μXRF). Table 1 shows the chemical compositions and the surface hardness for martensitic and austenitic NiTi workpieces.

The workpiece was mounted on the machining table using a customised fixture and bolted on a three-component Kistler Dynamometer Type 9256C. This dynamometer is connected to a laboratory charge amplifier and data acquisition system, KISTLER LabAmp Type 5167A, and linked to a host computer for force data collection. The force signal was sampled at 5000 Hz.

Table 1 Chemical compositions and hardness of workpiece

Types	Martensitic NiTi	Austenitic NiTi
Chemical compositions (at.%)	Ni: 55.93 Ti: 42.46 Fe: 1.61	Ni: 53.83 Ti: 46.17
Hardness (HV_1)	238	286
Types	Martensitic NiTi	Austenitic NiTi

The milling operation used a KRIS Vision two-flute 3-mm uncoated solid carbide end-mill tool with zero rake angle (Figure 1). Before the cutting process, the condition of the cutting tool was examined using Hitachi TM3000 Tabletop Scanning Electron Microscope (SEM). The milling experiments were performed using an Akira Seiki–Performa SR3 Computerised Numerical Control (CNC) Milling Machine. The setup for the milling process is shown in Figure 2.

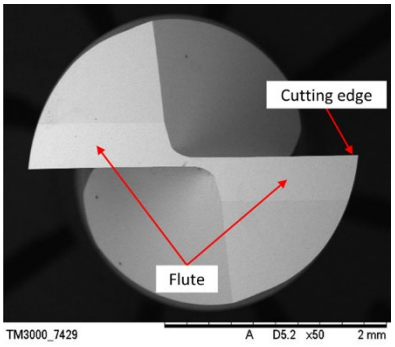

Figure 1 SEM image of the cutting tool

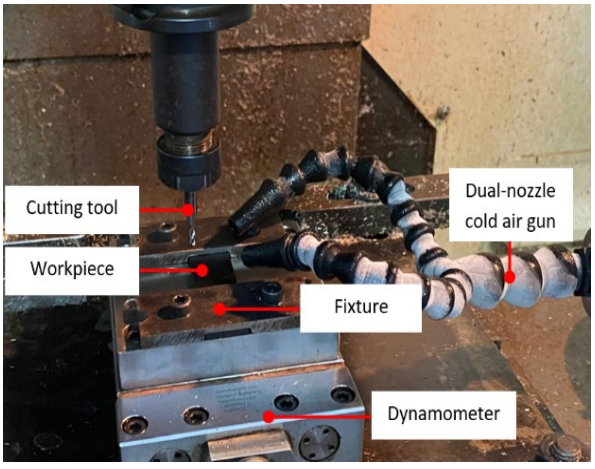

Figure 2 Experimental setup for the milling process

Based on optimum parameters established through pilot cutting tests, the spindle speed, feed rate and cutting depth were set at constant values of 5093 rpm, 509 mm/min and 0.18mm, respectively. The milling operations were run under two different cutting conditions: dry and chilled air cutting.

The chilled air condition was achieved using a VORTEC Adjustable Cold Air Gun System Type 610BSP supplied by VorTech UK. With a 6 mm-diameter dual nozzle type equipped to the cold air gun, a cold air stream of −14.5°C at a wind speed of around 14.0 m/s was produced.

Temperature measurement during cutting was made using a thermal imaging infrared camera, FLIR T440. The measurement temperature range for the thermal imaging infrared camera was set to −20°C to 120°C. The emissivity of the camera was set to 1, and the measuring distance was set to 1 metre. The surfaces of the workpieces were painted matte black to ensure the correct corresponding emissivity value of approximately 1, whereby the workpiece surfaces were focused for temperature measurement. The captured infrared images were analysed using FLIR Tools analyser software.

2.2 Methods and Data Collection

For the post-machining study of the tool wear, the images of the tool were captured using Hitachi TM3000 Tabletop SEM to identify the wear on the tools, while the quantification of the wear was done through ImageJ software. The tool wear was analysed in terms of flank wear based on the ISO 3685 standard. The burr formation on the NiTi workpieces was pictured using a Xoptron Stereo Microscope of model XST60, while the measurement of the burr (top burr) was done using IMT i-Solution Lite Imaging.

The Mitutoyo Surftest SJ-210 portable surface roughness checker was used to measure the workpieces' surface roughness values, Ra, which were measured five times for each machined surface, in accordance with the standard of ISO 4287. For differential scanning calorimetry (DSC) analysis, a TA Instruments Q20 Differential Scanning Calorimeter was used. Heating and cooling cycles were run with temperature ranges of –20°C to 120°C and –100°C to 100°C for the machined specimens of martensitic NiTi and austenitic NiTi, respectively. The heating-cooling rate used was 10°C/min. The tangent line interception method based on ASTM F2004-17 was used to determine the phase transformation temperatures of the NiTi materials.

Figure 3 shows the as-received DSC curves for martensitic NiTi and austenitic NiTi, respectively. For the as-received martensitic NiTi, the transformation temperatures of martensite start (M_s), martensite finish (M_f), austenite start (A_s), and austenite finish (A_f) temperatures were 70°C, 44°C, 75°C and 100°C, respectively. Meanwhile, for the as-received austenitic NiTi, the NiTi transformation temperatures were –26°C, –59°C, –22°C and 0°C for M_s, M_f, A_s, and A_f, respectively. These transformation temperatures are tabulated in Table 2.

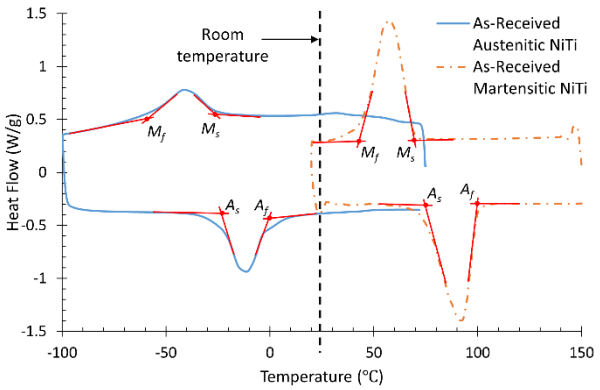

Figure 3 DSC curve of phase transformation temperatures of the as-received martensitic and austenitic NiTi

Table 2 Transformation temperatures of as-received NiTi

Transformation temperatures	M_s (°C)	M_f (°C)	A_s (°C)	A_f (°C)
Martensitic NiTi	70	44	75	100
Austenitic NiTi	–26	–59	–22	0

3.0 RESULTS AND DISCUSSION

3.1 Cutting Force

The resultant cutting force calculated for this study is shown in Figure 4. Based on the result, for the martensitic NiTi workpiece, the chilled air cutting produced a more significant resultant force with a reading of 23.7 N, the largest of all, compared to its dry cutting counterpart, which resulted in 14.5 N. This is surprising behaviour that is unexpected from the chilled air cutting.

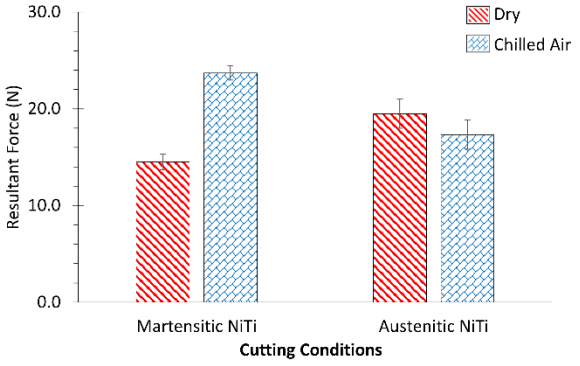

Figure 4 Cutting force for different cutting conditions

The higher force was produced due to the lower cutting temperature produced under chilled air [21]. The quenching effect was also introduced through the low-temperature chilled air, which hardened the workpiece and generated a higher cutting force. This showed that cutting force could increase due to the martensitic NiTi workpiece hardening, which surpassed the effect of friction reduction produced by chilled air.

Meanwhile, the chilled air cutting produced a lower resultant force for the austenitic NiTi workpiece, with a value of 17.3 N compared to that of dry cutting, which was 19.5 N. This was due to the action of pressurised air [22]. This pressurised air during chilled air cutting provided support for the lifting of sheared chip, which minimised the seizure area and friction coefficient. Eventually, this reflected in the reduction of resultant force during chilled air cutting of austenitic NiTi. This contradicts the phenomenon observed in martensitic NiTi. This contradicts the phenomenon observed in martensitic NiTi, where the adverse impacts of complex work hardening and thermomechanical behaviour of martensitic NiTi material were found to be superior to the impacts of friction reduction [23].

3.2 Cutting Temperature

This study calculated the average cutting temperature of the surface near the cutting tool (Figure 5). Figure 6 shows the comparisons of cutting temperatures under different cutting conditions. The dry cutting recorded a higher cutting temperature of 73°C and 87°C for martensitic and austenitic NiTi, respectively. The higher cutting temperature shown in dry cutting of austenitic NiTi was due to the higher hardness and strength of austenitic NiTi compared to martensitic NiTi. This led to higher deformation resistance for austenitic NiTi, causing higher temperature than martensitic NiTi.

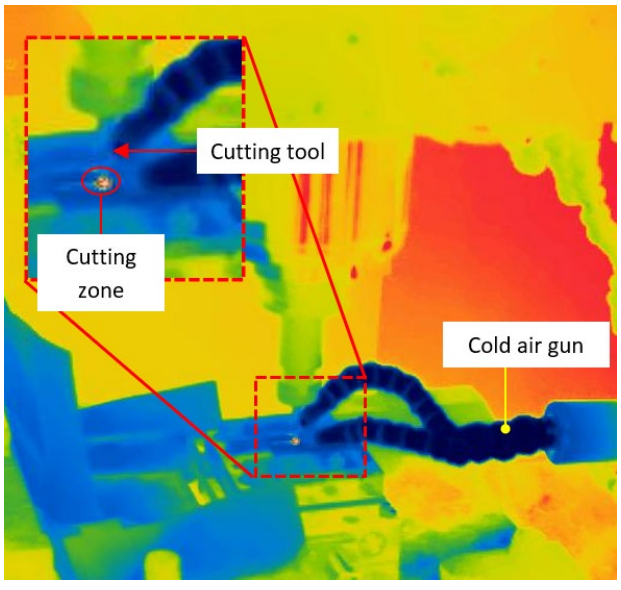

Figure 5 Infrared thermal image of chilled air milling

The chilled air condition lowered the cutting temperature to 52°C and 40°C for martensitic NiTi and austenitic NiTi, respectively. These are 28% and 54% reductions compared to their counterparts of dry cutting for martensitic (73°C) and austenitic NiTi (87°C), respectively. A higher reduction percentage was achieved in austenitic NiTi compared to martensitic NiTi. This is probably because martensitic NiTi has a higher ductility level than austenitic NiTi. The higher ductility can lead to a higher level of shearing force, consequently leading to some heat generated during machining, which prevents a further reduction of the cutting temperature during the chilled air cutting of martensitic NiTi.

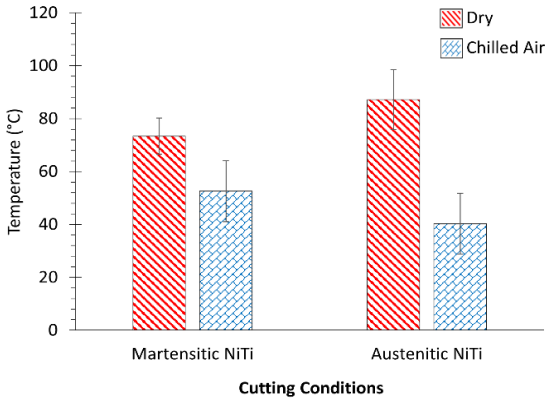

Figure 6 Cutting temperature variations under different cutting conditions

3.3 Tool Wear

Tool wear reflects the tool's effectiveness in removing material, where excessive wear leads to increased costs from frequent tool changes [24]. In this study, chilled air cutting demonstrated reduced tool wear compared to dry cutting, by limiting heat generation and preventing adhesion and build-up edge (BUE) formation. Several distinct wear modes were observed, including flank wear, material adhesion, BUE and chipping, as pictured in Figure 7.

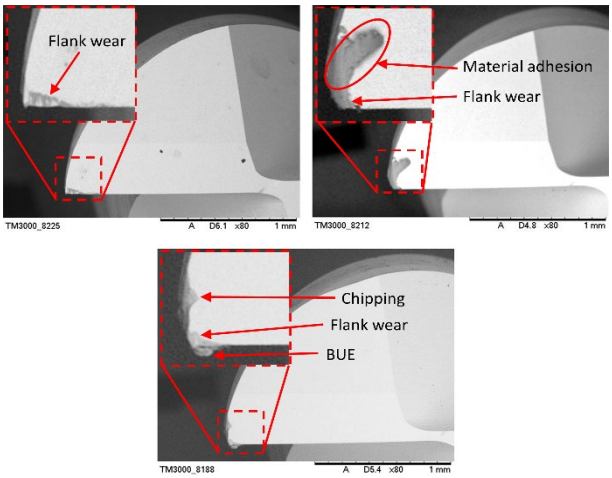

Figure 7 Different modes of tool wear

Among these modes of tool wear, flank wear, V_b was the most dominant occurrence of tool wear, as shown in Figure 8. The flank wear was found in dry and chilled air cutting for both austenitic and martensitic NiTi workpieces. In end-milling, the forces are primarily exerted through the end of the flank face, causing flank wear to intensify and progressively reduce the effective diameter of the cutting tool. Consequently, this flank wear condition will affect the dimensional precision and quality of the workpiece [25]. Thus, noting the importance of mitigating flank wear, flank wear has been the primary subject analysis in terms of tool wear in end-milling experiments [26], [27].

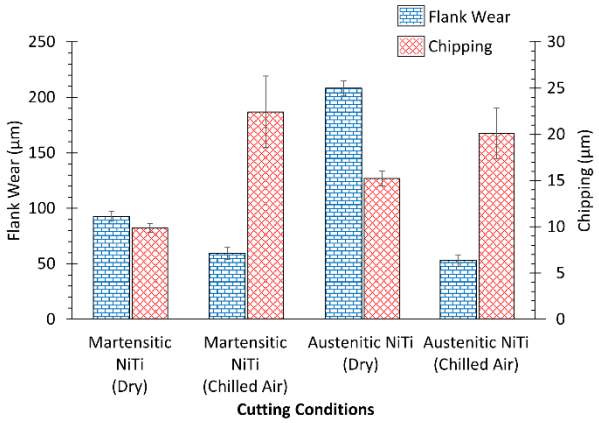

Figure 8 Comparison between flank wear and chipping

From Figure 9, the chilled air cutting shows observable reductions in tool wear in both NiTi workpieces, martensitic and austenitic NiTi. Based on Figure 10, the flank wear in chilled air cutting of martensitic NiTi was reduced by 36% to 60 µm from 93 µm in dry cutting. Meanwhile, in austenitic NiTi, the dry condition recorded flank wear of 208 µm, which is improved by 75% to 53 µm in chilled air condition. This is due to the chilled air cutting being able to lower the temperature in the cutting zone of the tool and workpiece interface [28]. Consequently, the overall tool wear under chilled air cutting was reduced due to the reduction of the heat-induced wear.

Meanwhile, dry cutting was found to cause severe wear in austenitic NiTi compared to martensitic NiTi. This is due to the austenitic NiTi workpiece having higher wear resistance compared to martensitic NiTi [29]. This higher wear resistance resulted from a harder austenitic phase that can resist more deformation compared to martensitic NiTi. This eventually increased the stress level applied to the tool during the dry cutting of austenitic NiTi, leading to increased tool wear. In addition, stress-induced martensite could also be formed in austenitic NiTi during milling operation, which can increase tool wear [30]. The dry cutting of austenitic NiTi also showed material adhesion effect on the tool. This is caused by high temperature, which promotes thermal softening interaction between the workpiece chip and the tool's flank face [31].

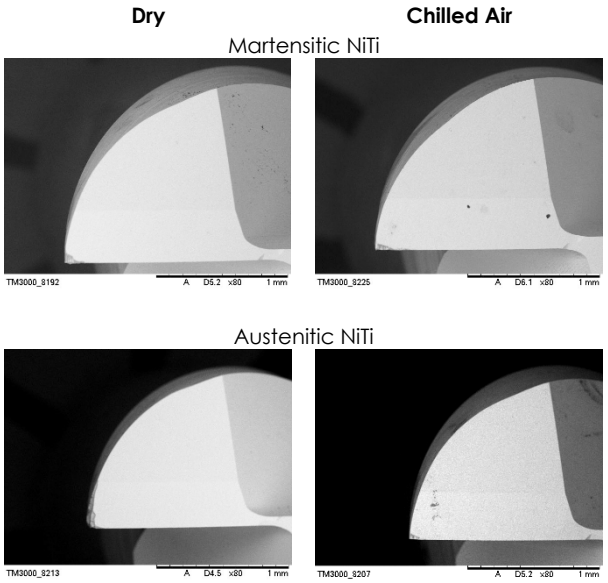

Figure 9 Tool wear under different cutting conditions

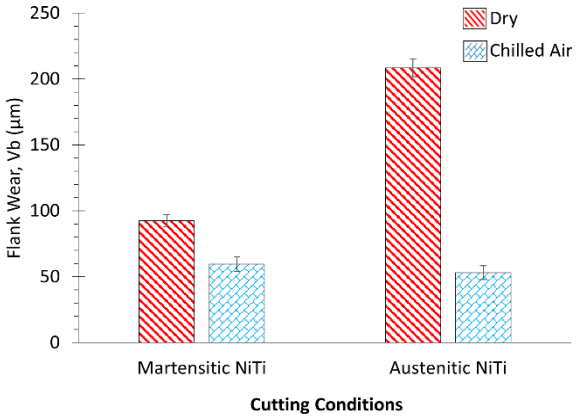

Figure 10 Flank wear under different cutting conditions

3.4 Burr Formation

Burr measurement is a considerable interest subject as it is interrelated to the performance and functionality of workpieces [32]. Low or minimised burr formation is a good indicator of a well-performed machining process. Analysing burr formation under different machining conditions can provide insight into understanding the relation between the cutting conditions and the workpiece materials. In this study, the top burr was measured in terms of its width using ImageJ software. Different shapes of tup burr were found, which include flocky shape, wavy shape and leaf shape, as shown in Figure 11.

From Figure 12, the dry cutting of martensitic NiTi recorded the largest average burr width of 530 µm, followed by austenitic NiTi dry cutting with 394 µm. The chilled air cutting yielded minimised burr width for both austenitic NiTi and martensitic NiTi with readings of 254 µm and 151 µm, respectively. Under dry cutting

of the martensitic NiTi, the poorest burr condition resulted due to the ductility effect of the martensitic NiTi, which was further enhanced by the thermal softening caused by the high temperature of dry cutting.

Meanwhile, both martensitic and austenitic NiTi show reading improvement under chilled air cutting compared to dry cutting. The impact of low-temperature air in chilled air cutting introduced brittleness into the NiTi material. The brittle condition of material consequently leads to easier break off during machining compared to ductile condition, which often leads to undesired burr protrusion due to its difficulty to fracture [33]. This shows the significance of choosing appropriate cutting conditions since proper coolant use could lower the temperature, which in turn affects the behaviour of materials during the formation of the burr.

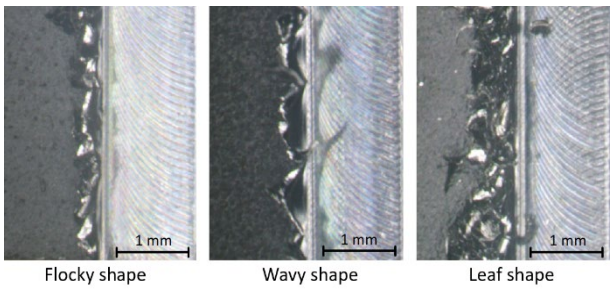

Figure 11 Different shapes of burr formation

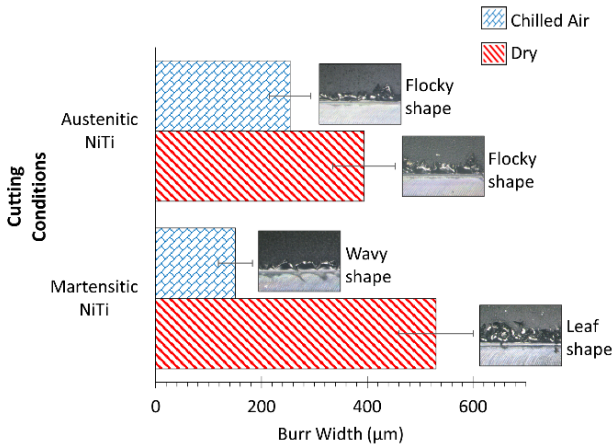

Figure 12 Burr width of machined NiTi

3.5 Surface Roughness

Surface roughness is a relevant subject to study in machining due to its relation to a product's fatigue life. Poor surface roughness is often associated with a high level of fatigue crack initiation life, which can be an introducing factor that leads to undesirable fatigue life, that needs to be avoided [34]. The surface roughness of the NiTi workpieces was determined using parameter R_a, the average calculated value of the surface's peaks and valleys.

Based on Figure 13, for martensitic NiTi, chilled air cutting recorded an average Ra of 0.348 µm, an improvement of 50% from a dry cutting condition, which recorded a Ra of 0.692 µm. Meanwhile, for austenitic NiTi, chilled air cutting resulted in an average Ra of 0.420 µm, a 20% improvement from a value of 0.527 µm in dry cutting.

This finding demonstrated better surface roughness under chilled air cutting compared to dry cutting due to the action of pressurised air [35]. Pressurised air in chilled air cutting can provide chip evacuation with minimal contact, potentially minimising the likelihood of micro-traces, leading to more uniform surface roughness. Besides, dry cutting might cause more heat that promotes rapid tool wear, eventually negatively affecting surface roughness [36].

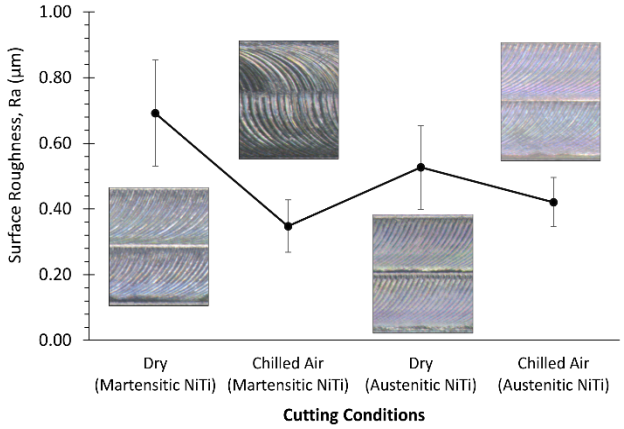

Figure 13 Surface roughness, R_a, under different cutting conditions

In comparing the surface roughness value under chilled air cutting between the two types of NiTi materials, the chilled air cutting of martensitic NiTi produced a slightly better result with R_a of 0.348 µm compared to chilled air cutting of austenitic NiTi, which recorded R_a of 0.420 µm. This difference in the outcome was attributed to the properties of the materials. Martensitic NiTi is known for its elevated level of ductility compared to austenitic NiTi. This higher ductility level eventually contributed to a lower surface roughness value due to the improved surface that was less affected by brittle fractures [37].

3.6 Transformation Temperatures

DSC is an analytical technique that compares and calculates the difference of heat or energy needed to elevate the temperature of a specimen sample and reference sample as a function of temperature [38]. This is important for identifying the occurrence of phase transformation in the specimen material. The thermal transition observed during DSC measurement provides valuable information that indicates the occurrence of phase transformation in the specimen material.

Figure 14 shows the DSC comparison of the martensitic NiTi between the as-received sample and the post-machining specimens cut under dry and chilled air cutting conditions. The DSC curves for martensitic NiTi machined under both cutting conditions were observed to be shifted compared to the as-received sample. Multiple martensite transformation peaks were observed for martensitic NiTi machined under dry and chilled air cutting. The M_f for dry cutting shifted to 40°C and 7°C for the first and second peak, respectively. Meanwhile, under chilled air cutting, the Mf shifted to 41°C and 20°C for the first and second peak, respectively, compared to the Mf of single-peak-martensite transformation for an as-received sample, which was 44°C.

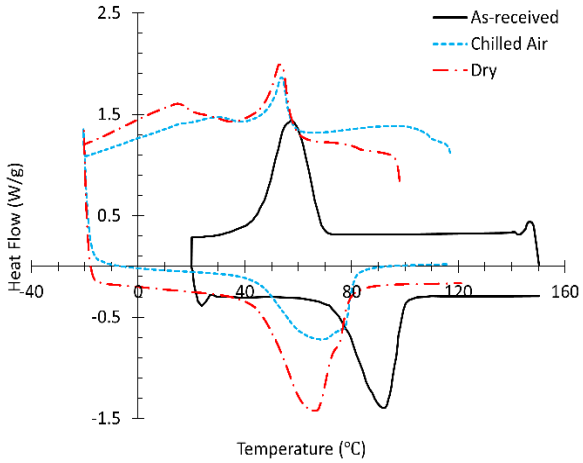

Figure 14 DSC curves of martensitic NiTi

The multiple peaks in the dry-cutting sample appear more vivid than those in the chilled air cutting of the martensitic NiTi. This is due to the high-temperature effect during dry cutting, which minimises dislocation during machining and promotes the inhibition of the martensitic transformation [39]. On the contrary, the chilled air cutting limits these temperature-induced effects, thus reducing the extent of microstructural alterations. This results in fewer changes in the DSC curve compared to dry cutting.

Based on Table 3, the austenitic transformation enthalpy (heating enthalpy) for the machined martensitic NiTi does not change significantly compared to the as-received state, which is maintained around 12 J/g. However, the martensitic transformation enthalpy (cooling enthalpy) of the post-machined martensitic NiTi samples show significant reduction compared to the as-received sample. This is due to the appearance of the second peak along the martensitic transformation path, inhibiting the completeness of phase transition and leading to lower enthalpy values [40].

For austenitic NiTi, the alteration of the DSC curve is shown in Figure 15, which compares the transformation enthalpy pathway of the as-received sample with those of post-machining samples machined under dry cutting and chilled air cutting.

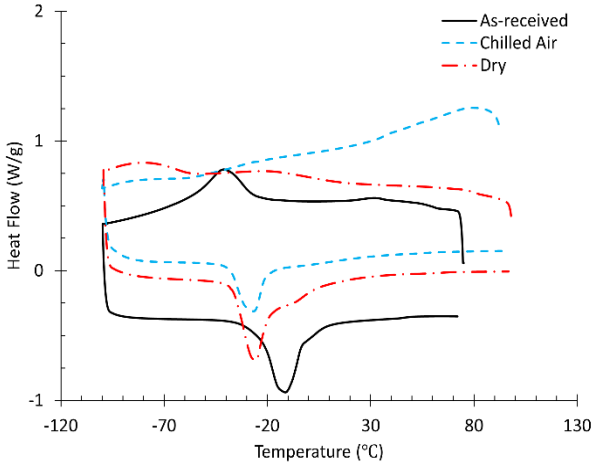

Figure 15 DSC curves of austenitic NiTi

The shifted peaks along the austenitic transformation path recorded reduction of transformation enthalpy compared to the as-received sample of the austenitic NiTi due to the heavy presence of R-phase in the austenitic NiTi materials [41]. This occurrence was due to the surface and subsurface damage and alteration that occurred, which were promoted by mechanical stresses and localised heating during machining. Eventually, the presence of R-phase was induced in the NiTi crystal structure, which disrupted and diminished the transformation enthalpy.

Table 3 DSC temperatures of transformation and transformation enthalpy of NiTi

Workpiece type	Cutting conditions	Martensite transformation				Austenite transformation		$\Delta H^{A\rightarrow M}$ (J/g) cooling	$\Delta H^{M\rightarrow A}$ (J/g) heating
		Peak 1st		Peak 2nd					
		M_s (°C)	M_f (°C)	M_s (°C)	M_f (°C)	A_s (°C)	A_f (°C)		
Martensitic NiTi	As-received	70	44	–	–	75	100	13.51	12.86
	Dry	61	40	22	7	43	80	3.43	12.11
	Chilled air	59	44	39	16	47	82	2.60	12.06
Austenitic NiTi	As-received	–26	–59	–	–	–22	0	4.56	7.70
	Dry	–	–	–	–	–41	3	–	5.66
	Chilled air	–	–	–	–	–40	–10	–	3.51

4.0 CONCLUSION

This study investigated the machining impacts of two major types of NiTi alloys—martensitic NiTi and austenitic NiTi—by analysing key machinability aspects, including cutting force, tool wear, burr formation, and surface roughness. Additionally, phase transformation characteristics were examined through Differential Scanning Calorimetry (DSC) analysis. The results showed that chilled air cutting did not significantly reduce the cutting force for martensitic NiTi compared to dry cutting. In the machining of austenitic NiTi, chilled air cutting demonstrated a notable reduction in the resultant cutting force compared to dry cutting. Overall, chilled air cutting reduced the cutting temperature more effectively than dry cutting. The lowest average temperature recorded under chilled air cutting was 40°C, demonstrating its superior cooling capability. Additionally, better tool wear resistance and lower burr formation were observed in chilled air cutting compared to dry cutting. In martensitic NiTi machining, chilled air cutting achieved the lowest tool wear (59.7 µm) and minimal burr formation (151 µm), outperforming dry cutting. Utilising chilled air also improved surface roughness, yielding Ra values of 0.348 µm (martensitic NiTi) and 0.420 µm (austenitic NiTi). Compared to dry cutting, these values represent improvements of 50% for martensitic NiTi and 20% for austenitic NiTi. Neither chilled air nor dry cutting significantly reduced alterations in the NiTi transformation curves. However, chilled air cutting mitigated the inhibition of multi-peak appearances in martensitic NiTi machining, potentially offering better phase stability.

Acknowledgement

This research is fully supported by the FRGS grant, FRGS/1/2023/TK10/UNIMAP/02/10. The authors fully acknowledge the Ministry of Higher Education (MOHE) and Universiti Malaysia Perlis (UniMAP) for the approved funds, which make this important research possible and effective.

Conflicts of Interest

The authors declare that there is no conflict of interest that could have appeared to influence the work reported in this paper.

References

[1] Abedini, M., Ghasemi, H. M., & Nili Ahmadabadi, M. 2009. Tribological Behavior of Niti Alloy in Martensitic and Austenitic States. *Materials and Design*. 30(10): 4493–4497. https://doi.org/10.1016/j.matdes.2009.05.031.

[2] Aslantas, K., Hasçelik, A., Erçetin, A., Danish, M., Alatrushi, L. K. H., Rubaiee, S., & Bin Mahfouz, A. 2024. Effect of Cutting Conditions on Tool Wear and Wear Mechanism in Micro-Milling of Additively Manufactured Titanium Alloy. *Tribology International*. 193. https://doi.org/10.1016/j.triboint.2024.109340

[3] Benedicto, E., Carou, D., & Rubio, E. M. 2017. Technical, Economic and Environmental Review of the Lubrication/Cooling Systems Used in Machining Processes. *Procedia Engineering*. 184: 99–116. https://doi.org/10.1016/j.proeng.2017.04.075.

[4] Chaudhary, K., Haribhakta, V. K., & Jadhav, P. V. 2024. A Review of Shape Memory Alloys in MEMS Devices and Biomedical Applications. *Materials Today: Proceedings*. https://doi.org/10.1016/j.matpr.2024.04.105.

[5] Danesh, N., Mahmoodabadi, M. J., & Fathi, A. R. 2023. Investigation of the Damping Performance of a Shape Memory Alloy Beam. *International Journal of Engineering, Transactions B: Applications*. 36(7): 1369–1382. https://doi.org/10.5829/ije.2023.36.07a.17.

[6] Debnath, S., Reddy, M. M., & Yi, Q. S. 2014. Environmental Friendly Cutting Fluids and Cooling Techniques in Machining: A Review. *Journal of Cleaner Production*. 83: 33–47. https://doi.org/10.1016/j.jclepro.2014.07.071.

[7] Deng, B., Peng, F., Zhou, L., Wang, H., Yang, M., & Yan, R. 2020. A Comprehensive Study on Flank Wear Progression of Polycrystalline Diamond Micro-Tool during Micro End-Milling of Sicp/Al Composites. *Wear*. 456: 203291. https://doi.org/10.1016/j.wear.2020.203291.

[8] Elahinia, M. H., Hashemi, M., Tabesh, M., & Bhaduri, S. B. 2012. Manufacturing and Processing of NiTi Implants: A Review. *Progress in Materials Science*. 57(5): 911–946. https://doi.org/10.1016/j.pmatsci.2011.11.001.

[9] Gao, S., Duan, X., Zhu, K., & Zhang, Y. 2024. Investigation of the Tool Flank Wear Influence on Cutter-Workpiece Engagement and Cutting Force in Micro Milling Processes. *Mechanical Systems and Signal Processing*. 209. https://doi.org/10.1016/j.ymssp.2024.111104.

[10] Iasniia, V., Sobaszek, L., & Yasniy, P. 2022. Study of Cyclic Response of SMA Based Damping Device. *Procedia Structural Integrity*. 36: 284–289. https://doi.org/10.1016/j.prostr.2022.01.036.

[11] Jin, S. Y., Pramanik, A., Basak, A. K., Prakash, C., Shankar, S., & Debnath, S. 2020. Burr Formation and Its Treatments—A Review. *International Journal of Advanced Manufacturing Technology*. 107(5–6): 2189–2210. https://doi.org/10.1007/s00170-020-05203-2.

[12] Kapuria, S., & Das, H. N. 2018. Improving Hydrodynamic Efficiency of Composite Marine Propellers in Off-Design Conditions using Shape Memory Alloy Composite Actuators. *Ocean Engineering*. 168: 185–203. https://doi.org/10.1016/j.oceaneng.2018.09.001.

[13] Katna, R., Suhaib, M., & Agrawal, N. 2020. Nonedible Vegetable Oil-Based Cutting Fluids for Machining Processes–A Review. *Materials and Manufacturing Processes*. 35(1): 1–32. https://doi.org/10.1080/10426914.2019.1697446.

[14] Kaynak, Y., Karaca, H. E., & Jawahir, I. S. 2014. Surface Integrity Characteristics of Niti Shape Memory Alloys Resulting from Dry and Cryogenic Machining. *Procedia CIRP*. 13: 393–398. https://doi.org/10.1016/j.procir.2014.04.067.

[15] Machado, R., & Sencadas, V. 2017. Advanced Techniques for Characterizing Bioinspired Materials. *Bioinspired Materials for Medical Applications*. 177–214. https://doi.org/10.1016/B978-0-08-100741-9.00007-3.

[16] Masood Arif Bukhari, S., Husnain, N., Arsalan Siddiqui, F., Tuoqeer Anwar, M., Abbas Khosa, A., Imran, M., Hassan Qureshi, T., & Ahmad, R. 2023. Effect of Laser Surface Remelting on Microstructure, Mechanical Properties and Tribological Properties of Metals and Alloys: A Review. *Optics and Laser Technology*. 165: 109588. https://doi.org/10.1016/j.optlastec.2023.109588.

[17] Mehta, K., & Gupta, K. 2019. Machining of Shape Memory Alloys. *SpringerBriefs in Applied Sciences and Technology*. 9–37.

https://doi.org/10.1007/978-3-319-99307-2_2
[18] Ninarello, D., Passaretti, F., & Nespoli, A. 2023. Body Temperature Niti Alloys: Effect of the Heat Treatment on the Functional Thermo-Mechanical Properties. *Journal of Thermal Analysis and Calorimetry*. 148(20): 10757–10775. https://doi.org/10.1007/s10973-023-12437-1
[19] Nipanikar, S. R., Sonawane, G. D., & Sargade, V. G. 2023. Tool Life of Uncoated and Coated Inserts during Turning of Ti6Al4V-ELI under Dry and Minimum Quantity Lubrication Environments. *International Journal of Engineering, Transactions A: Basics*. 36(2): 191–198. https://doi.org/10.5829/ije.2023.36.02b.01
[20] Zailani, Z. A., Rosli, M. H., Zailani, Shuaib, N. A., Zainuddin, M. Z., & Azawqari, A. A. 2025. Optimisation of Cutting Performance in Drilling of Aluminium Alloy 7075 Involving Chilled Air Cooling Under Taguchi Method. *Journal of Advanced Research in Applied Mechanics*. 133(1): 12–23. https://doi.org/10.37934/aram.133.1.1223
[21] Pimenov, D. Y., Mia, M., Gupta, M. K., Machado, Á. R., Pintaude, G., Unune, D. R., Khanna, N., Khan, A. M., Tomaz, Í., Wojciechowski, S., & Kuntoğlu, M. 2022. Resource Saving by Optimization and Machining Environments for Sustainable Manufacturing: A Review and Future Prospects. *Renewable and Sustainable Energy Reviews*. 166: 112660. https://doi.org/10.1016/j.rser.2022.112660
[22] Khan, M. A., Mia, M., & Dhar, N. R. 2017. High-Pressure Coolant on Flank and Rake Surfaces of Tool in Turning of Ti-6Al-4V: Investigations on Forces, Temperature, and Chips. *The International Journal of Advanced Manufacturing Technology*. 90: 1977-1991. https://doi.org/10.1007/s00170-016-9511-6.
[23] Wang, Z., Luo, J., Kuang, W., Jin, M., Liu, G., Jin, X., & Shen, Y. 2022. Strain Rate Effect on the Thermomechanical Behavior of NiTi Shape Memory Alloys: A Literature Review. *Metals*. 13(1): 58. https://doi.org/10.3390/met13010058.
[24] Rahman, M., Senthil Kumar, A., & Ling, M. S. 2003. Effect of Chilled Air on Machining Performance in End Milling. *Int J Adv Manuf Technol*. 21: 787–795. https://doi.org/10.1007/s00170-002-1394-z.
[25] Shahir Kasim, M., Ngah, N., Bahri Mohamed, S., Abdul Rahman, Z., Hassan Che Haron, C., Nurul Akmal Yusof, S., Ghani, J. A., & Mohamad, A. 2023. Machining Surface Quality Evaluation of Inconel 718: A Comparative Study of Various Coolant and Lubrication Strategies in Milling Process. *Jurnal Tribologi*. 39:17–35. https://doi.org/10.1016/j.rineng.2022.100764.
[26] Shokrani, A., Dhokia, V., & Newman, S. T. 2012. Environmentally Conscious Machining of Difficult-To-Machine Materials with Regard to Cutting Fluids. *International Journal of Machine Tools and Manufacture*. 57: 83–101. https://doi.org/10.1016/j.ijmachtools.2012.02.002.
[27] Singh, G., Aggarwal, V., & Singh, S. 2020. Critical Review on Ecological, Economical and Technological Aspects of Minimum Quantity Lubrication Towards Sustainable Machining. *Journal of Cleaner Production*. 271: 122185. https://doi.org/10.1016/j.jclepro.2020.122185.
[28] Sun, Y., Sun, J., Li, J., Li, W., & Feng, B. 2013. Modeling of Cutting Force under the Tool Flank Wear Effect in End Milling Ti6Al4V with Solid Carbide Tool. *International Journal of Advanced Manufacturing Technology*. 69(9–12): 2545–2553. https://doi.org/10.1007/s00170-013-5228-y.
[29] Sureshkumar, B., Navaneethakrishnan, G., Panchal, H., Manjunathan, A., Prakash, C., Shinde, T., Mutalikdesai, S., & Prajapati, V. V. 2024. Effects of Machining Parameters on Dry Turning Operation of Nickel 200 Alloy. *International Journal on Interactive Design and Manufacturing*. 18(8): 6023–6038. https://doi.org/10.1007/s12008-023-01442-1.
[30] Tanzi, M. C., Farè, S., & Candiani, G. 2019. Biomaterials and Applications. *Foundations of Biomaterials Engineering*. 199–287. https://doi.org/10.1016/B978-0-08-101034-1.00004-9.
[31] Yip, W. S., & To, S. 2018. Ductile and Brittle Transition Behavior of Titanium Alloys in Ultra-Precision Machining. *Scientific Reports*. 8(1): 3934. https://doi.org/10.1038/s41598-018-22329-2.
[32] Lei, Y., Gao, J., Xu, Z., Guo, B., Wang, M., Zhong, W., Zeng, W. & Xu, X. 2025. Study on the Formation Mechanism and Morphology of Edge Burrs in Radial Fly-Cutting of Triangular Pyramid Microstructures. *Journal of Materials Research and Technology*. 36: 727–735. https://doi.org/10.1016/j.jmrt.2025.03.091.
[33] Zailani, Z. A., & Mativenga, P. T. 2016. Effects of Chilled Air on Machinability of NiTi Shape Memory Alloy. *Procedia CIRP*. 45: 207–210. https://doi.org/10.1016/j.procir.2016.02.156.
[34] Wang, X., Huang, C., Zou, B., Liu, G., Zhu, H., & Wang, J. 2018. Experimental Study of Surface Integrity and Fatigue Life in the Face Milling of Inconel 718. *Frontiers of Mechanical Engineering*. 13: 243–250. https://doi.org/10.1007/s11465-018-0479-9.
[35] Zailani, Z. A., Rusli, N. S. N., & Shuaib, N. A. 2021. Effect of Cutting Environment and Swept Angle Selection in Milling Operation. *International Journal of Engineering, Transactions B: Applications*. 34(12). https://doi.org/10.5829/IJE.2021.34.12C.02.
[36] Zainal Abidin, Z., Tarisai Mativenga, P., & Harrison, G. 2020. Chilled Air System and Size Effect in Micro-milling of Nickel−Titanium Shape Memory Alloys. *International Journal of Precision Engineering and Manufacturing - Green Technology*. 7(2): 283–297. https://doi.org/10.1007/s40684-019-00040-5.
[37] Nath, C., Zhang, X., Senthil Kumar, A., & Rahman, M. 2014. Ultrasonic Vibration Cutting: Part II: Ductile Cutting and Analytical Force Models for the Elliptical Vibration Cutting Process. *Comprehensive Materials Processing*. 13(11): 455–481. https://doi.org/10.1016/B978-0-08-096532-1.01328-5.
[38] Zhao, Y., Guo, K., Li, J., & Sun, J. 2021. Investigation on Machinability of Niti Shape Memory Alloys under Different Cooling Conditions. *The International Journal of Advanced Manufacturing Technology*.1913–1923. https://doi.org/10.1007/s00170-021-07563-9.
[39] Zhu, J.N., Borisov, E., Liang, X., Huizenga, R., Popovich, A., Bliznuk, V., Petrov, R., Hermans, M. & Popovich, V. 2022. Controlling Microstructure Evolution and Phase Transformation Behavior in Additive Manufacturing of Nitinol Shape Memory Alloys by Tuning Hatch Distance. *Journal of Materials Science*. 57(10): 6066-6084. https://doi.org/10.1007/s10853-022-07007-z.
[40] Zhao, Y., Li, J., Guo, K., Sivalingam, V., & Sun, J. 2020. Study on Chip Formation Characteristics in Turning Niti Shape Memory Alloys. *Journal of Manufacturing Processes*. 58: 787–795. https://doi.org/10.1016/j.jmapro.2020.08.072.
[41] Zhao, Y. Z., Guo, K., Sivalingam, V., Li, J. F., Sun, Q. D., Zhu, Z. J., & Sun, J. 2021. Surface Integrity Evolution of Machined Niti Shape Memory Alloys after Turning Process. *Advances in Manufacturing*. 9(3): 446–456. https://doi.org/10.1007/s40436-020-00330-1.